HAL
open science

Effect of kappa carrageenan on acid-induced gelation of whey protein aggregates. Part II: Microstructure

Dasong Liu, Peng Zhou, Taco Nicolaï

To cite this version:

Dasong Liu, Peng Zhou, Taco Nicolaï. Effect of kappa carrageenan on acid-induced gelation of whey protein aggregates. Part II: Microstructure. Food Hydrocolloids, 2020, 102, pp.105590. 10.1016/j.foodhyd.2019.105590 . hal-03026673

HAL Id: hal-03026673

https://hal.science/hal-03026673v1

Submitted on 3 Dec 2020

HAL is a multi-disciplinary open access archive for the deposit and dissemination of scientific research documents, whether they are published or not. The documents may come from teaching and research institutions in France or abroad, or from public or private research centers.

L'archive ouverte pluridisciplinaire **HAL**, est destinée au dépôt et à la diffusion de documents scientifiques de niveau recherche, publiés ou non, émanant des établissements d'enseignement et de recherche français ou étrangers, des laboratoires publics ou privés.

Effect of Kappa Carrageenan on Acid-induced Gelation of Whey Protein Aggregates. Part II: Microstructure

Dasong Liu[a,b], Peng Zhou[a], Taco Nicolai[b,*]

[a]*State Key Laboratory of Food Science and Technology, Jiangnan University, Wuxi, Jiangsu Province 214122, China*

[b]*Le Mans Université, IMMM UMR-CNRS 6283,* Polymères, Colloïdes et Interfaces, *72085 Le Mans cedex 9, France*

Email: Taco.nicolai@univ-lemans.fr

Abstract

The influence of κ-carrageenan (KC) was investigated on the microstructure of gels formed by acid-induced gelation of whey protein aggregates (WPA). In part I of this two-part series we discussed results obtained by potentiometric titration, rheology and turbidimetry. Here we report on the microstructure of both the proteins and the polysaccharides using confocal laser scanning microscopy with different fluorescent labels for each type of biopolymer. The effect of KC concentration at fixed net protein charge densities (α) and the effect of α at fixed KC concentrations were studied. It is shown that WPA starts to form microdomains and associates with KC at approximately the same α. Microstructures at steady state at different α were compared with those obtained at different times during in-situ acidification after addition of GDL. Significantly different microstructures were observed at elevated gelation temperatures. Fluorescence recovery after photobleaching measurements showed that a significant fraction of the KC chains associated with the proteins could still freely exchange even when the proteins were strongly positively charged. The observations of the microstructure are compared with those obtained with other experimental techniques that were reported in part I.

Keywords κ-carrageenan; whey protein; complex; gel; microstructure

1. Introduction

Gelation of proteins is an important method to texture food products. Often polysaccharides are present as well as proteins. Polysaccharides can form gels by themselves, but even if they don't gel themselves they may still influence the gelation process of the proteins and thereby influence the texture of the food products. Polysaccharides can also be added on purpose in order to obtain a more desirable texture. It is therefore of importance to investigate the interaction between proteins and polysaccharides during gelation of the former. Native globular proteins in aqueous solution can form a gel when they are denatured, which is usually done by heating (Brodkorb, Croguennec, Bouhallab and Kehoe, 2016; Nicolai, 2019) . However, suspensions of globular proteins aggregates formed by preheating can be induced to form a gel by reducing the electrostatic interactions even at low temperatures (Bryant and McClements, 1998; Kharlamova, Chassenieux and Nicolai, 2018; Kharlamova, Nicolai and Chassenieux, 2018) , which is useful for certain applications.

We have conducted an extensive investigation of the influence of adding the anionic polysaccharide κ-carrageenan (KC) on the acid-induced gelation of whey protein aggregates (WPA). By decreasing the pH the strongly net negative charge density of the proteins is reduced, which drives association of the WPA, and if the protein concentration is sufficiently high, a self supporting gel is formed. Elsewhere, we reported on potentiometric titration, rheology and turbidimetry measurements, which we refer to as part I (Liu, Zhou, Nicolai, 2020). We showed with potentiometric titration that addition of KC strongly influences the relationship between the pH and the net charge of the proteins (α) for $\alpha > -2$, due to the formation of complexes between the proteins and KC. We note that complexation occurred even if WPA and KC have both a net negative charge. It is important to realize that the parameter that controls the interaction between the biopolymers is α and not the pH. The value of α was varied in-situ by adding glucono-δ-lactone (GDL) and can be deduced from the amount of added GDL and measurements of the pH as was described in detail in part I.

Oscillatory shear measurements showed that gels were formed starting at a critical charge density and that gelation was accompanied by increase of the turbidity. Adding more than 1 g/L KC to 20 g/L WPA led to a strong decrease of the gel stiffness and a strong increase of the turbidity. The effect of the temperature was also investigated and showed that stiffer and more turbid gels were formed at higher temperatures. The gelation rate increased strongly with increasing temperature and was controlled by the degradation rate of GDL, i.e. the rate at which α changed. Confocal scanning microscopy (CLSM) images of acid-induced

WPA gels in the presence of KC reported in the literature (de Jong and van de Velde, 2007) showed that the presence of KC induced formation of gels with a coarser microstructure. This can explain the increase of the turbidity in the presence of KC. It was speculated that the effect of KC on WPA gelation was caused by segregative microphase separation between KC chains and the associating WPA followed by binding of KC to the WPA network.

However, in earlier studies of the microstructure of the mixed gels only the proteins were visualized. Here we report on the microstructure of the gels using CLSM with different fluorescent labels for the proteins and the polysaccharides, which allowed us to localize each biopolymer in the mixtures. In this manner we were able to assess if and to what extent microphase separation has occurred and importantly how much KC is co-localized with the proteins as a function of α and time. Co-localization doesn't imply that the polysaccharides are actually strongly bound. Therefore, fluorescence recovery after photobleaching (FRAP) measurements were done, which allowed us to determine the fraction of strongly bound immobile KC.

2. Materials and Methods

For the preparation and characterization of the WPA and the KC samples we refer to part I. Briefly, mixtures of WPA and KC were prepared from stock solutions at the desired concentration. A GDL solution at 1 M was prepared by adding water to the GDL powder. After stirring for 1 min to dissolve all the GDL powder, aliquots of the GDL solution were added to the biopolymer solutions while stirring. The values of α at steady state were calculated using the relationship between the pH and α established by potentiometric titration measurements that were reported in part I. The proteins were physically labelled by adding a small amount of Rhodamin B. The polysaccharides were covalently labelled with FITC following the method described by Heilig et al. (Heilig, Göggerle and Hinrichs, 2009) with minor modifications as described by Bui et al. (Bui, Nguyen, Nicolai and Renou, 2019) . The molar mass of the KC was not significantly modified by the labelling.

2.1. CLSM and FRAP

Mixtures of WPA and KC with a small fraction of labelled KC were prepared from stock solutions and subsequently the required amount of GDL was added as described in part I. The solutions were inserted between a concave slide and a cover slip that were hermetically

sealed with an adhesive Gene Frame® (ABgene®, Epsom, UK). CLSM observations were made at 20°C with a Zeiss LSM800 (Jena, Germany). The images with a pixel size of 70 nm were obtained with a 63x water immersion objective with a numerical aperture of 1.3. It took 0.3 s to obtain one image. An excitation wavelength of 561 nm and detection wavelengths above 550 nm were used for the Rhodamine B channel, whereas an excitation wavelength of 488 nm and detection wavelengths below 520 nm were used for the FITC channel. The concentration of labelled KC added in all cases was 0.25 g/L. At this small concentration of labelled KC the microstructure observed with the protein signal was the same as without labelled KC at the same total KC concentration. Care was taken not to saturate the detection so that the measured intensity was proportional to the biopolymer concentration.

Histograms of the fluorescence intensity distribution were obtained using the Image-J programme and the relative standard deviation was calculated as the standard deviation divided by the average intensity. The standard deviation of the histograms depends on the overall intensity of the images, which in terms depends on the gain, laser intensity and fluorescent probe concentration. However, normalizing the standard deviation by the average intensity of the images renders it independent of these parameters and only a function of the microstructure. The ratio of the intensities of the pores and the network was obtained by measuring the intensity of many small circular areas with a diameter of 5 µm in different parts of the pores and the protein network. Care was taken to sample only within the protein network sections that were in focus and to minimalize the inclusion of edges.

FRAP measurements were done following the method of Bui et al. (2019) with minor modifications. Circular areas with diameter w = 10 µm were bleached and the recovery of the fluorescence intensity with time of the area was measured. One pre-bleach image and one bleach image were taken followed by 6 post-bleach images at time intervals of 5 s, 6 images at time intervals of 50 s and 11 images at time intervals of 500 s. In this manner the recovery was probed on a logarithmic time scale. Consecutive imaging with very short time intervals (0.3 s) of non-bleached images showed that no significant bleaching occurred during detection of the recovery.

3. Results and Discussion

3.1 Effect of the KC concentration

The effect of the KC concentration up to 6 g/L on the microstructure of the protein gels at steady state was studied for gels formed in the presence of 9 mM GDL at C_{WP}=20 g/L.

At this concentration of GDL the steady state value of α was close to zero and very little dependent on the KC concentration, whereas the pH varied between 4.9 and 5.1. Fig. 1 compares CLSM images formed at 20°C or 80°C, but visualized at 20°C. The turbidity of gels formed at 80°C did not change during cooling to 20°C and it is therefore reasonable to assume that the structure observed at 20°C is the same as at 80°C where it was formed. At both temperatures the heterogeneity of the gels increased with increasing KC concentration until about 1 g/L, but adding more KC did not appear to have a significant influence on the microstructure. For $C_{KC} \geq 1$ g/L the gels appear to consist of approximately spherical domains that are crosslinked into a network. The effect of KC on the microstructure shown in figure 1 is similar to that shown by (de Jong and van de Velde, 2007) for gels formed at 20°C, at C_{WP} = 30 g/L and at a fixed pH 4.8. Interestingly, the transition to the formation of microdomains corresponds approximately to the transition between dilute and semi-dilute KC solutions (Croguennoc, Meunier, Durand and Nicolai, 2000) .

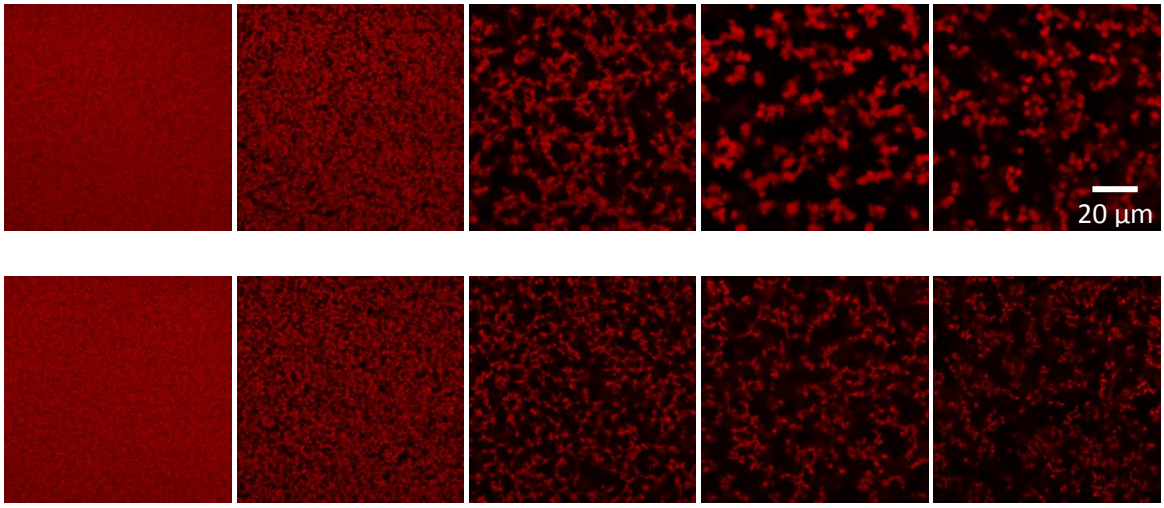

0 g/L 0.25 g/L 1 g/L 2 g/L 6 g/L

Fig. 1 CLSM images of gels formed after heating at 20°C (top) and 80°C (bottom) by mixtures of 20 g/L WPA and different KC concentrations. The steady state value of α was close to zero. The fluorescence of the proteins is indicated by the bright (red) colouring.

One method to quantify the heterogeneity of the microstructure is to calculate the histogram of the fluorescence intensities. They show a broadening with increasing KC

concentration and for $C_{KC} \geq 1$ g/L the histogram splits between a narrow high amplitude distribution at $I/I_{mean} < 1$ and a broad low amplitude distribution in the range $I/I_{mean} = 1 - 5$, see Figure 2a. This implies that for $C_{KC} \geq 1$ g/L phase separation has occurred on length scales accessible to CLSM In Figure 2b we compare the dependence of the standard deviation of the histograms normalized by the mean intensity (σ_{rel}) as a function of C_{KC} for gels formed at 20°C and at 80°C. σ_{rel} increased steeply with increasing KC concentration up to 1.5 g/L and then remained constant. Up to $C_{KC} = 1$ g/L the effect of temperature was weak, but at higher KC concentrations, σ_{rel} was larger for gels formed at 20°C.

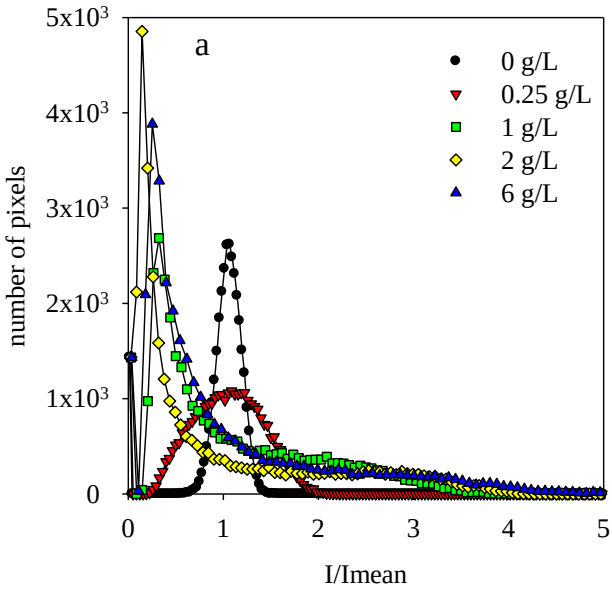

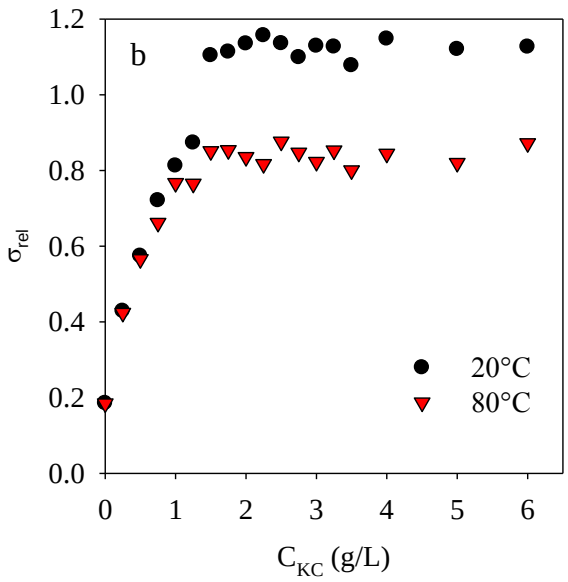

Fig. 2a Histograms of the fluorescence intensity relative to the average intensity for gels of the images shown in fig. 1.

Fig. 2b Comparison of the dependence of the relative standard deviation, i.e. the standard deviation of the intensity histogram normalized by the mean intensity, on the KC concentration for gels formed at 20°C and 80°C.

3.2 Effect of the temperature

The effect of the temperature on the microstructure of the gels was explored in more detail for mixtures containing 1, 2 and 4 g/L KC. Figure 3 shows CLSM images for mixtures at C_{KC} = 2 g/L formed at different temperatures. They confirm the impression that the gel structure becomes less heterogeneous when formed at higher temperatures. Figure 4 shows that σ_{rel} dropped sharply above 50 °C both at C_{KC} = 2 g/L and 4 g/L, but was almost independent of the temperature at C_{KC} = 1 g/L. The results also show that the structure becomes independent of the KC concentration for $C_{KC} \geq 1.5$g/L at all temperatures. De Jong et al. (2009) compared the microstructure of gels at C_{WP} = 30 g/L formed at 25°C and 37°C in the presence of 5 g/L KC and found very little difference in agreement with the present results. However, here we find that for C_{KC} > 1 g/L there is a significant effect of the temperature above 50°C leading to formation of smaller protein domains.

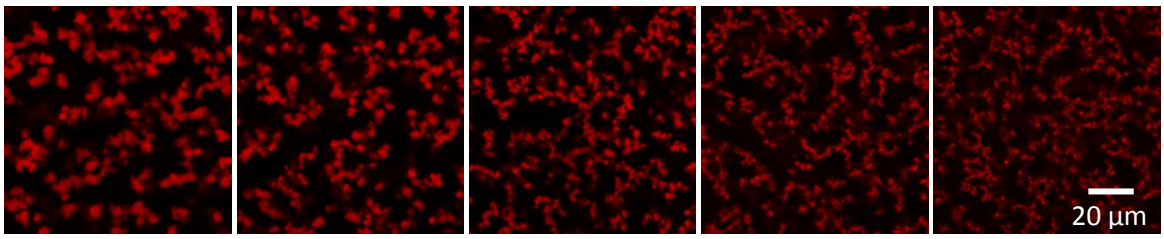

20°C 35°C 50°C 65°C 80°C

Fig. 3 CLSM images of gels formed after heating at different temperatures by mixtures of 20 g/L WPA and 2 g/L KC. The steady state value of α was close to zero.

In part I we showed that the gel stiffness increased significantly with increasing gelation temperature for $C_k \geq 2$ g/L. Here we find that smaller microdomains were formed at higher temperatures suggesting that the two phenomena are related. However, whereas the gel

stiffness increased progressively with increasing gelation temperature, the microstructure changed only significantly above 50 °C. It is therefore not straightforward to relate the gel stiffness to the microstructure. We note that the turbidity at C_{KC} = 2 g/L actually increased with increasing temperature, see figure 12a of part I, whereas the size of the microdomains decreased. This illustrates that the relationship between the turbidity and the microstructure as probed by CLSM is not straightforward.

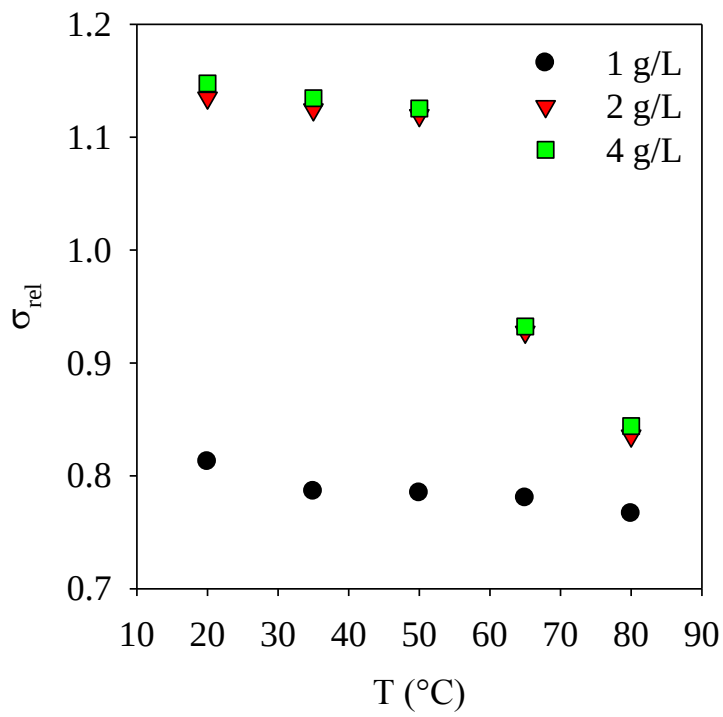

Fig.4 Dependence of the relative standard deviation, i.e. the standard deviation of the intensity histogram normalized by the mean intensity, on the temperature of gelation for gels formed by mixtures of 20 g/L WPA and different KC concentrations. The steady state value of α was close to zero.

3.3 Complexation between KC and WPA

A crucial issue is whether and to what extent KC binds to the protein gel. As was mentioned in the introduction, titration measurements show a clear influence of the presence of KC for α > - 2.0, which indicates that complexes are formed between the two types of

biopolymers. However, this measurement cannot show the extent to which KC is bound to the protein gels at different α. KC can be localized within the gels using CLSM by covalently labelling KC with a fluorescent probe different from the one used to label the protein and its fluorescence was detected at different wavelengths.

Figure 5 shows CLSM images of mixtures of 20 g/L WPA and 2 g/L KC that have reached steady state at 20°C after addition of different amounts of GDL corresponding to different steady state values of α. The correspondence between α and the pH was shown in part I. The microstructures of the proteins and KC was visualized separately and compared. At α = - 3.6 the microstructure of both biopolymers was homogeneous on length scales accessible to CLSM. At α = - 3.3, protein rich domains could be observed, but KC still appeared homogeneously distributed. At α = - 3.0 the protein network structure was distinctly visible and the same network structure could also be seen with the signal corresponding to KC implying that KC was bound to the proteins. However, still much of the KC was homogeneously distributed. As α was further increased a larger fraction of KC became bound to the protein network. This visual impression is confirmed by co-localisation plots of the KC signal vs the protein signal, see Figure S1 of the supplementary information.

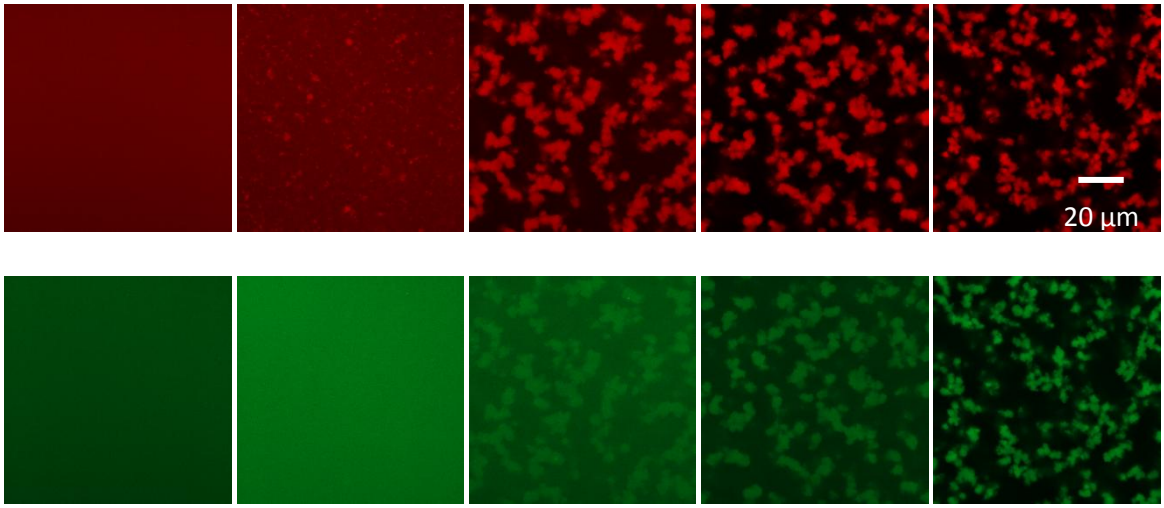

-3.6 -3.3 -3.0 -2.0 0.1

Fig. 5 CLSM images of gels formed at 20°C after adding different amounts of GDL resulting in different steady state values of α indicated in the figure. The distribution of proteins indicated in red is shown in the top row and that of KC indicated in green is shown in the bottom row.

The fact that the KC is co-localized with the protein domains implies attractive interaction between the two biopolymers that is strong enough to overcome the mixing entropy that drives KC to be homogeneously distributed. We do not believe that the attractive interaction is caused by the labeling of KC as the protein microstructure was the same as with unlabelled KC. Furthermore, binding of KC was progressive with increasing α and we showed elsewhere that KC with the same labelling actually segregated from the protein domains at neutral pH (Nguyen, B. T., Nicolai, T., Chassenieux, C. & Benyahia, L. (2014)).

The dependence of σ_{rel} on α for the proteins and KC is compared in Figure 6. Below $\alpha = -3.3$, the CLSM images were visually homogeneous with values of σ_{rel} between 0.12 and 0.22. For the proteins σ_{rel} started to increase strongly with increasing α at $\alpha = -3.3$, which is caused by the association of WPA and formation of a heterogeneous gel. This initial steep increase was followed by a weak increase for $\alpha > -2.4$. The protein structure is strongly influenced by the presence of KC at all α as σ_{rel} remains small in the absence of KC, see Figure 6. If all KC is bound to the protein, σ_{rel} should be the same for both biopolymers. This is clearly not the case as σ_{rel} corresponding to KC increased much more progressively with α and approaches the value of the proteins only at large α.

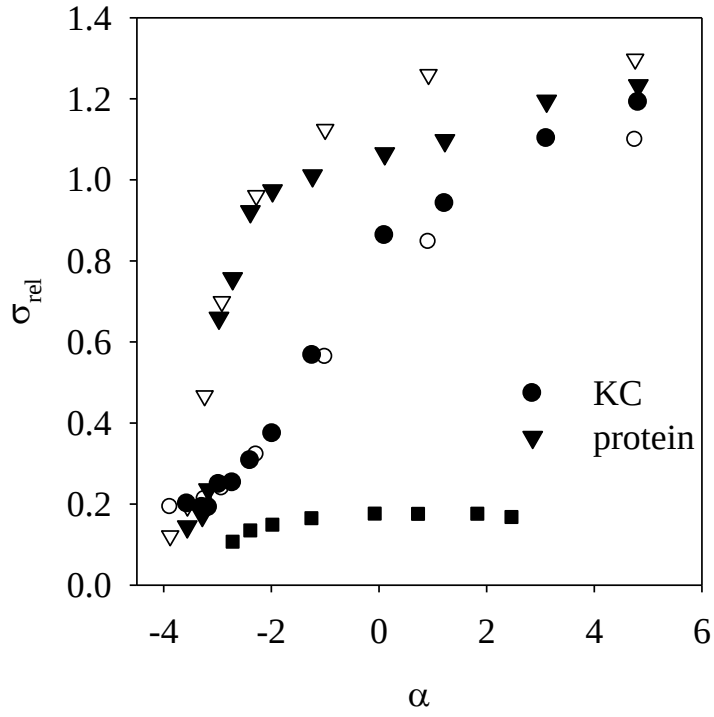

Fig.6 Dependence on the net protein charge density of the relative standard deviation of the protein (triangles) and KC (circles) intensity distributions for mixtures of 20 g/L WPA and 2 g/L KC at steady state after addition of different amounts of GDL (filled symbols). Results derived from the time dependence, see text, are shown as open symbols. For comparison the relative standard deviations obtained for pure protein gels are also shown (squares).

For a more direct measure of the partition of each biopolymer between the gel and the sol fraction, we measured the ratio (R) of the intensity in the pores over that of the network. The assumption is that all fluorescent probes are bound to the biopolymers and that the sol fraction within the network structure is negligible. The dependence of R on α is shown in figure 7. R was unity for the proteins at α = -3.6 where no dense domains could be detected, but it decreased steeply with increasing α to R = 0.05 at α = -2. For KC, R started to decrease at the same value of α, but the decrease was more progressive reaching a value of 0.1 at α = 0.1. At α = -2.4, when the protein network was already fully formed and contained almost all of proteins, R was still as high as 0.6 for KC, i.e. most of the KC was still free in solution.

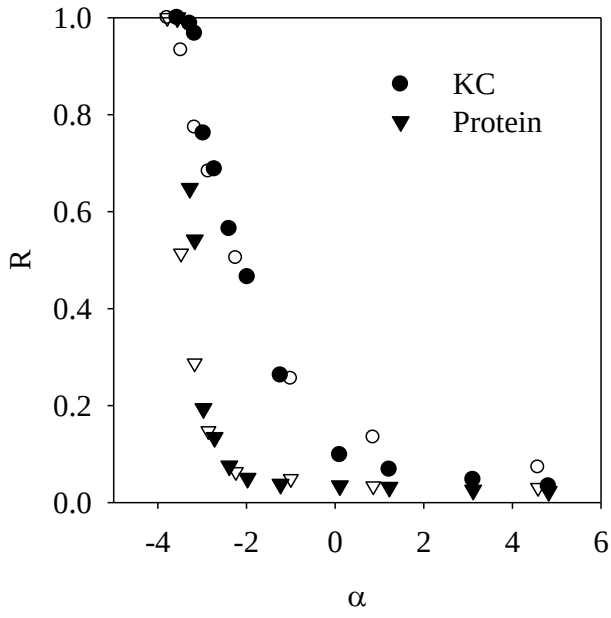

Fig. 7 Dependence on α of the ratio of the protein and KC fluorescence intensities in the sol and the gel phase for mixture of 20 g/L WPA and 2 g/L KC at steady state after addition of different amounts of GDL (filled symbols). Results derived from the time dependence, see text, are shown as open symbols.

We may compare these results with rheology and turbidity results reported in part I. The rise in the turbidity started at the same value of α as where σ_{rel} increased and was caused by the formation of the microdomains. The increase of the storage shear modulus also started at approximately the same value of α, which means that the critical value of α where microdomains are formed and where these domains start to connect into a space filling network are very close.

The effect of the KC concentration on the partition of the biopolymers in gels formed at 20°C was investigated at $\alpha \approx 3$ where the values of σ_{rel} for the protein and polysaccharide signal were close at C_{KC} = 2 g/L and R was small for both biopolymers. CLSM images showed a similar dependence of the microstructure on the KC concentration at $\alpha \approx 3$ as at α = 0, see figure 8. Comparison of the protein and KC signals shows that at this charge density the KC was co-localized with the proteins at all KC concentrations. This was confirmed by the values of σ_{rel} that were close for both biopolymers and the low values of R for both biopolymers, see figure 9. However, whereas the values of σ_{rel} for the proteins remained

approximately the same, σ_{rel} of the KC signal decreased weakly between 4 and 6 g/L KC and R increased by a factor two from 0.05 to 0.1. The titration measurements discussed in part I suggest that for C_{KC} > 4 g/L the proteins started to become saturated with KC, which may explain why more free KC was observed within the pores.

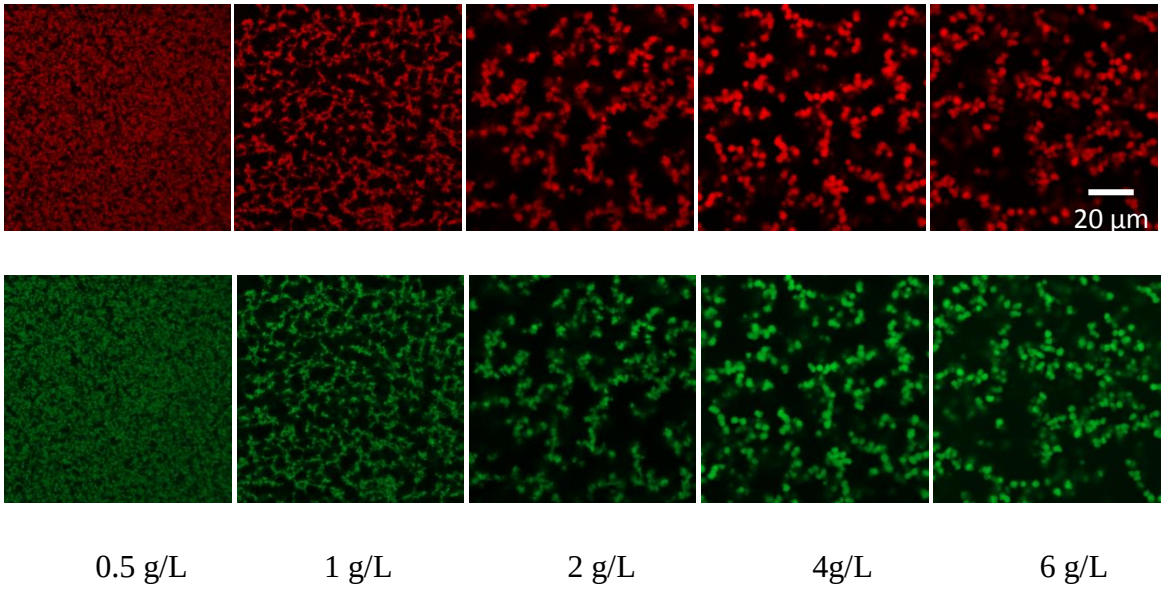

Fig. 8 CLSM images of mixtures of 20 g/L WPA and different concentrations of KC at α≈ 3.0. The distribution of proteins indicated in red is shown in the top row and that of KC indicated in green is shown in the bottom row.

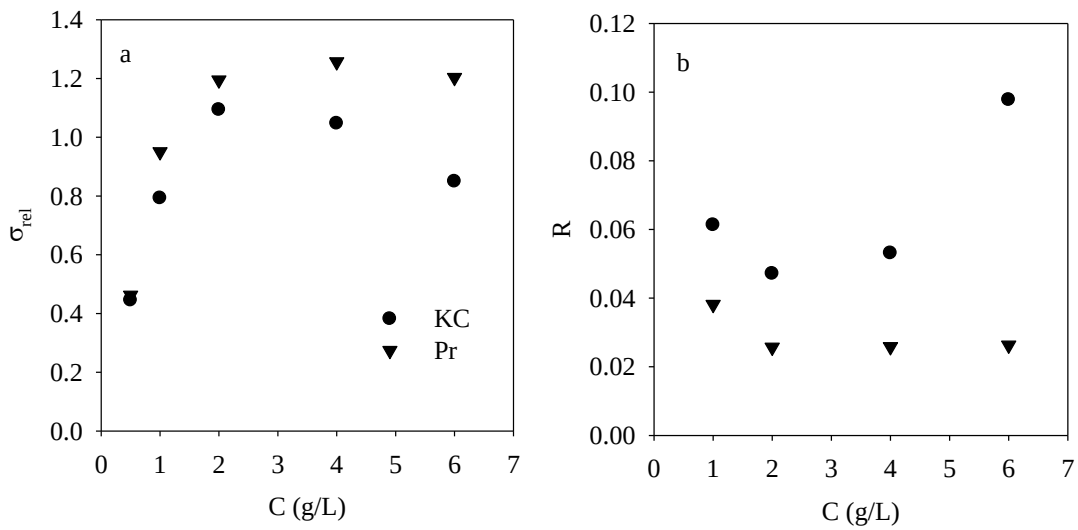

Fig.9 Dependence of the relative standard deviation of the protein and the KC intensity distributions (a) and the ratio of the protein and the KC intensity in the sol and the gel phase (b) on the KC concentrations at $\alpha \approx 3.0$.

In part I we showed that the turbidity increased steeply up to C_{KC} = 1 g/L, but remained approximately constant at higher concentrations. Here we find that the microstructure changes strongly with increasing KC concentrations until C_{KC} = 1 g/L and remains the same at higher concentrations, see figure 1, in agreement with the turbidity measurements. However, the stiffness of the gels did not vary much with increasing KC concentration until C_{KC} = 1 g/L and decreased steeply only at higher concentrations. It is clear that the gel stiffness is not directly related to the microstructure and that one needs to consider the effect on the connectivity and the bond strength as well, which is influenced by the presence of KC.

3.4 Evolution of the microstructure during gelation

As was mentioned in the introduction, the formation of a more heterogeneous protein structure in the presence of KC has been attributed to segregative phase separation between the associating WPA aggregates and KC that is arrested by gelation (De Jong et al., 2009) . However, it is clear from the measurements shown above that at steady state the concentration of KC in the protein rich domains is not lower than that in the protein poor domains at any α, which contradicts segregative phase separation. Nevertheless, one may wonder if segregative phase separation occurs during the gelation process. Therefore we studied the evolution of the microstructure in-situ with CLSM during degradation of GDL. Figure 10 shows the evolution of the protein and KC microstructure as a function of time at 20°C for a mixture containing 20 g/L WPA and 2 g/L KC. A relatively large quantity of GDL was added (22 mM) in order to ensure fast gelation. Up to 55 min, the distribution of both biopolymers was homogeneous. After 60 min, small dense protein domains were visible, whereas KC was still homogeneously distributed. After 65 min, more protein was assembled in the form of dense domains that were connected into a network. KC showed the same structure implying that KC and protein were co-localized. At longer times the network structure no longer evolved much. The important conclusion that can be drawn from this experiment is that at no time during the gelation process does segregative phase separation occur between the protein aggregates and KC. However, close to the critical value of α the WPA/KC complexes are dispersed in a semi-

dilute solution of free excess KC, which could drive phase separation between the complexes and excess KC via depletion interaction.

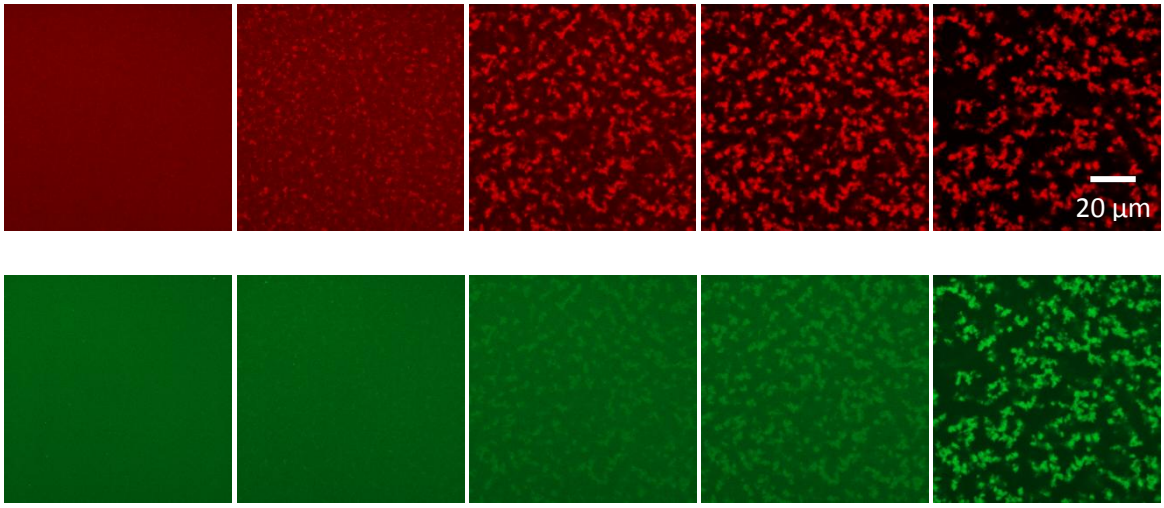

55 min 60 min 65 min 70 min 100 min

Fig. 10 CLSM images of mixtures of 20 g/L WPA and 2 g/L KC at different times after addition of 22 mM GDL. The distribution of proteins indicated in red is shown in the top row and that of KC indicated in green is shown in the bottom row.

Similar measurements were done at C_{KC} = 1 and 4 g/L. The evolution of σ_{rel} is shown in figure 11. For the proteins, σ_{rel} increased sharply at a characteristic time (t_c) and then stabilized. t_c decreased weakly with increasing KC concentration in agreement with the weak decrease of the critical time where the turbidity started to increase shown in figure 11 of part I. The values of σ_{rel} at long times increased with increasing KC concentration in agreement with the steady state values shown in figure 2. For KC, σ_{rel} increased progressively with time and approached the same values as for the proteins only at long times.

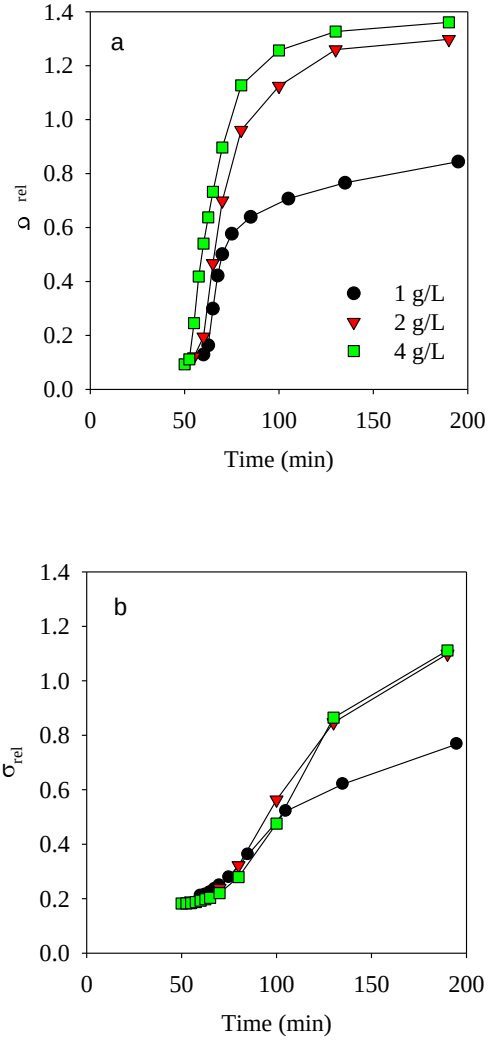

Fig. 11 Evolution of the relative standard deviation with time after addition of 22 mM GDL for the protein structure (a) and KC (b) for mixtures of 20 g/L WPA and different concentrations of KC indicated in the figure.

The evolution of the contrast in fluorescence between the pores and the network is shown in figure 12. R started to decrease at the same time for both biopolymers, but the decrease was much steeper for the proteins. It is clear that all KC is not bound immediately to the proteins, but that an increasing fraction of KC binds progressively with time to the proteins. These results as a function of time are strikingly similar to those as a function of α shown in figures 6 and 7. In part I we have shown that α is proportional to the amount of degraded GDL for $\alpha < 2$ and that the fraction of degraded GDL increases linearly with time up to a fraction of 0.5. It took 170 min to degrade half of the GDL, i.e. 11 mM in this

experiment. We may consider that in the relevant range of α the increase of α is proportional to the amount of degraded GDL. It follows that α increased at a rate of 0.058 × t, with t in minutes. Titration measurements of WPA showed that the initial value of α was -7.4 ±0.2, see part I. Good quantitative agreement between the dependence on time and on α at steady state was obtained if we use α(t) = -7.2 + 0.062t, see figs 6 and 7, which is close to the calculated time dependence of α. The good superposition implies that the rate at which the microstructure evolves is limited by the evolution of α.

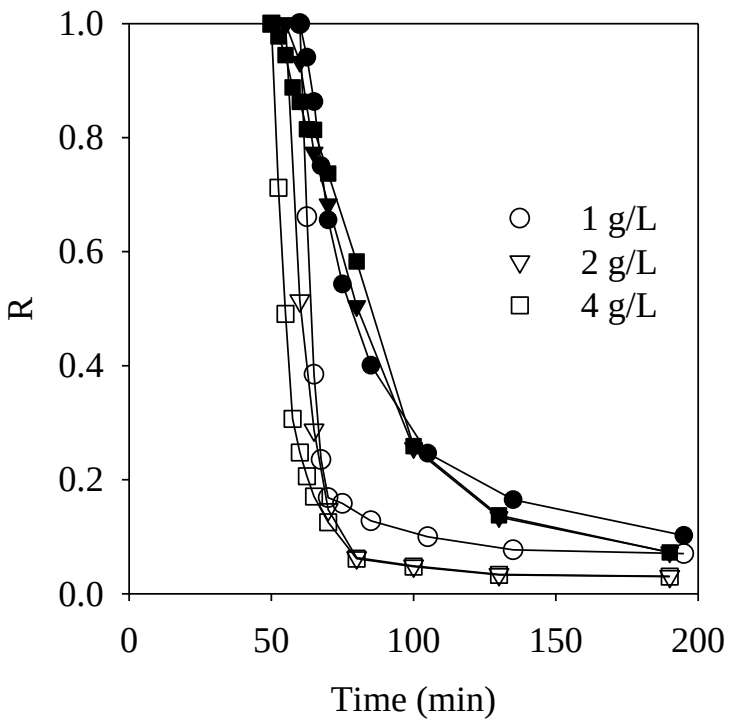

Fig.12 Evolution of R with time after addition of 22 mM GDL for the proteins (open symbols) and KC (filled symbols) for mixtures of 20 g/L WPA and different concentrations of KC indicated in the figure.

3.5 Mobility of KC chains

We have shown above that KC becomes increasingly co-localized with the proteins with increasing α. However, CLSM images cannot show to what extent the polysaccharides are bound to the proteins or can exchange with polysaccharides elsewhere. The exchange can be probed using FRAP by bleaching small circular areas with diameter w = 10 μm situated in

the network. As an example images of a gel before bleaching and at different times after bleaching is shown in Figure S2 of the supplementary information. The fluorescence recovery (F(t)) was calculated from the time dependent intensity (I(t)) as: $F(t) = (I(t)-I(0))/(I_{int}-I(0))$, where I_{int} is the intensity before bleaching and I(0) is the intensity just after bleaching. Figure 13 shows examples of F for gels formed by mixtures of 20 g/L WPA and 2 g/L KC at different α. The solid line in figure 13 shows the predicted recovery for the case that it is caused by diffusion motion of the labelled chains with a single diffusion coefficient (D):

$$F(t) = \exp(-2\tau/t)[I_0(2\tau/t)+I_1(2\tau/t)] \qquad 1$$

where $\tau = w^2/4D$ is the characteristic time needed to diffuse out of the bleached area and I_0 and I_1 are Bessel functions (Soumpasis, 1983) . At α = -3.6 the recovery was complete and could be described in terms of a single diffusion coefficient ($D = 1.9 \times 10^{-11}$ m^2/s) indicating that the KC chains where not bound to protein domains. However, this was clearly not the case at larger α. The initial increase of F can still be described by eq. 1 with the same relaxation time, if we assume that only a fraction of KC moves freely, see solid lines in figure 13. However, this initial fast recovery is followed by a very slow increase of F on logarithmic time scales. A similar behaviour has recently been reported for dextran chains in heat-set whey protein gels (Inthavong, Nicolai and Chassenieux, 2018) .

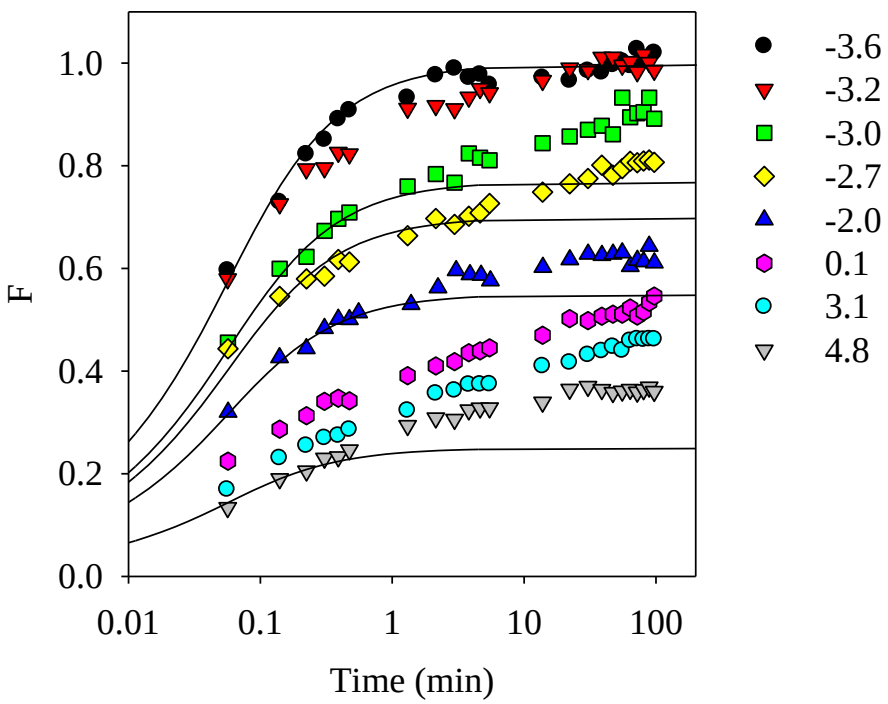

Fig. 13 Recovery of the KC fluorescence intensity for mixtures of 20 g/L WPA and 2 g/L KC at different values of α indicated in the figure. Solid lines correspond to eq. 1 with D = 1.9 $\times 10^{-11}$ m^2/s.

The value of F reached after 100 min ((F(100)) decreased sharply with increasing α starting at α = -3.2 followed by a weak decrease for α > -1.5, see figure 14. Notice that the fraction of KC that diffused unhindered was less and decreased down to about 20% at α = 4.8. Figure 7 shows that at α > 0 the KC concentration associated with the protein network was more than 10 times larger than in the sol so that the contribution to F of KC in the sol can be neglected. We may therefore conclude that a significant fraction of the KC that was associated with the protein network remained fully mobile even at large α. Obviously, more work is needed in order to elucidate the mechanism of binding and release of KC chains to the protein network.

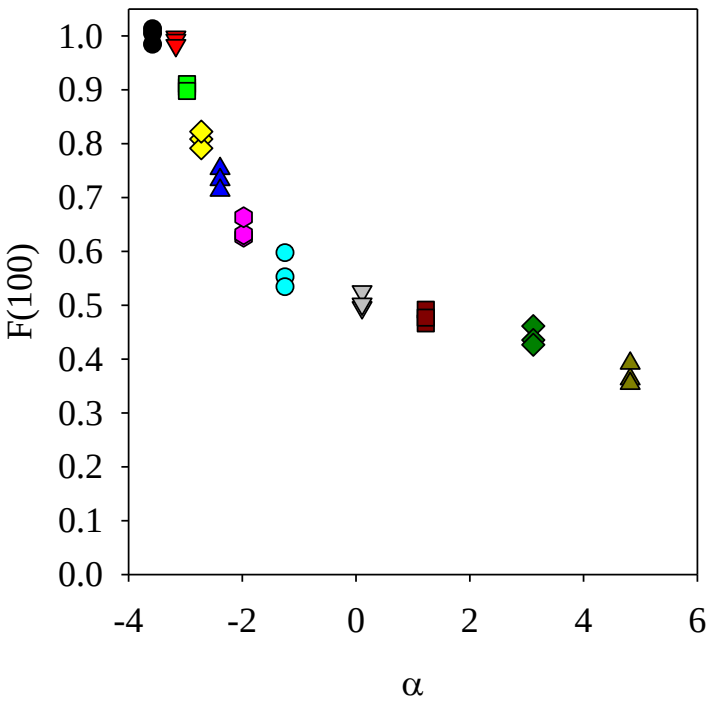

Fig. 14 Recovery of the KC fluorescence intensity after 100 min for mixtures of 20 g/L WPA and 2 g/L KC as a function of α. Results are shown of measurements at three different spots in the network of each gel.

3.6 Gelation mechanism

CLSM images of the proteins and KC fluorescence show that acidification does not induce segregative phase separation between KC and WPA aggregates at any value of α. Instead dense protein domains are formed that contain at least as much KC as in the protein poor phase. The rate at which the microstructure is formed is set by the rate at which GDL degrades and therefore results as a function of α are the same whether they are obtained by measuring the dependence on time or on the GDL concentration at steady state. The important implication is that the microstructures observed at different α are not caused by phase separation between KC and growing WPA that was arrested by gelation. The presence of KC led to the formation of dense protein microdomains, but KC was not expelled from these domains. In fact, binding of KC to the proteins started at the same α as where the domains were formed.

We therefore propose the following scenario, see figure 15. Reduction of the net negative charge density of the proteins below a critical value allows the WPA aggregates to bind to each other and some of the KC chains become associated with the proteins. If enough KC is present, free excess KC is depleted from between protein/polysaccharide complexes which drives the formation of microdomains by the complexes. This process is facilitated by reduction of the electrostatic repulsion between the complexes as α is increased. The complexes within the microdomains crosslink so that they transform into microgels. These microgels initially do not cluster together due to residual electrostatic repulsion. If α is increased further more microgels are formed and a larger fraction of KC binds to the proteins. In addition, the electrostatic repulsion between the microgels decreases further causing them to cluster into large flocs at C < 10 g/L and to form a system spanning network at higher protein concentrations. A significant fraction of the KC that is associated with the proteins is free to exchange and another fraction can exchange very slowly, indicating that the KC chains are associated with the protein network with a variety of conformations and bond strengths.

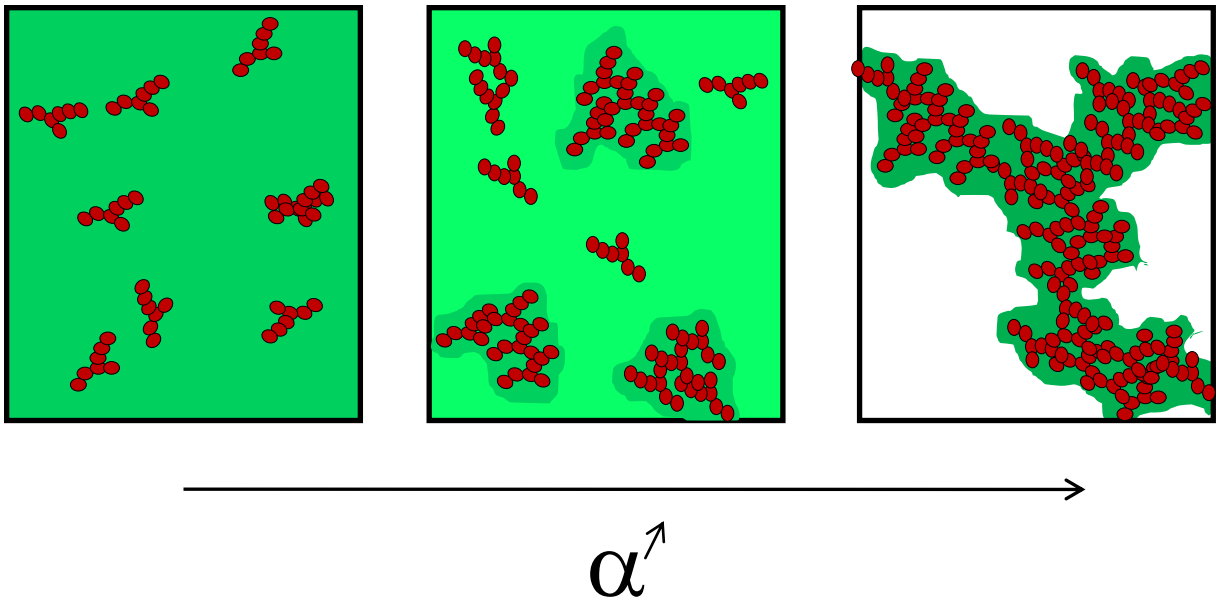

Fig. 15 Schematic representation of mixtures of WPA and KC as a function of α. The protein aggregates are indicated in red and the distribution of the KC chains is indicated in green.

4. Conclusion

In the presence of semi-dilute solutions of KC, whey protein aggregates spontaneously assemble into microdomains when their net negative charge density is decreased below a critical value. Concomitantly, KC starts to bind to positive patches on the proteins and forms complexes. The WPA aggregates in the microdomains connect to each other and to the KC chains to form microgels. As the net negative charge decreases further the microgels crosslink and form a space filling network and progressively more KC becomes associated with the protein network. Most of the KC that is associated with the network is strongly bound when the proteins have a net positive charge density, but a significant fraction of associated KC remains mobile.

The changes in the gel morphology as a function of time after addition of GDL is determined by the rate at which GDL degrades. The rate of GDL degradation increases strongly with increasing temperature, which leads to the formation of gels with smaller domain sizes above 50°C presumably because microdomains have less time to develop before they crosslink.

Acknowledgements

This research was partly supported by the National Natural Science Foundation of China (31901613), the China Postdoctoral Science Foundation (2018M640457) and the Jiangsu Province Postdoctoral Science Foundation (2018K089C).

References

Brodkorb, A., Croguennec, T., Bouhallab, S. & Kehoe, J. J. (2016). Heat-Induced Denaturation, Aggregation and Gelation of Whey Proteins, *Advanced Dairy Chemistry*(pp. 155-178), Springer

Bryant, C. M. & McClements, D. J. (1998), Molecular basis of protein functionality with special consideration of cold-set gels derived from heat-denatured whey, *Trends in Food Science & Technology*, **9**, 143-151.

Bui, V. T. N. T., Nguyen, B. T., Nicolai, T. & Renou, F. (2019), Mobility of carrageenan chains in iota- and kappa carrageenan gels, *Colloids and Surfaces A: Physicochemical and Engineering Aspects*, **562**, 113-118.

Croguennoc, P., Meunier, V., Durand, D. & Nicolai, T. (2000), Characterization of semidilute κ-carrageenan solutions, *Macromolecules*, **33**, 7471-7474.

De Jong, S., Klok, H. J. & Van de Velde, F. (2009), The mechanism behind microstructure formation in mixed whey protein-polysaccharide cold-set gels, *Food Hydrocolloids*, **23**, 755-764.

de Jong, S. & van de Velde, F. (2007), Charge density of polysaccharide controls microstructure and large deformation properties of mixed gels, *Food Hydrocolloids*, **21**, 1172-1187.

Heilig, A., Göggerle, A. & Hinrichs, J. (2009), Multiphase visualisation of fat containing β-lactoglobulin-κ-carrageenan gels by confocal scanning laser microscopy, using a novel dye, V03-01136, for fat staining, *LWT - Food Science and Technology*, **42**, 646-653.

Inthavong, W., Nicolai, T. & Chassenieux, C. (2018), Polymer Probe Diffusion in Globular Protein Gels and Aggregate Suspensions, *The Journal of Physical Chemistry B*, **122**, 8075-8081.

Kharlamova, A., Chassenieux, C. & Nicolai, T. (2018), Acid-induced gelation of whey protein aggregates: Kinetics, gel structure and rheological properties, *Food Hydrocolloids*, **81**, 263-272.

Kharlamova, A., Nicolai, T. & Chassenieux, C. (2018), Calcium-induced gelation of whey protein aggregates: Kinetics, structure and rheological properties, *Food Hydrocolloids*, **79**, 145-157.

Liu, D., Zhou, P., Nicolai, T. (2020), Effect of Kappa Carrageenan on Acid-induced Gelation of Whey Protein Aggregates. Part I: Potentiometric Titration, Rheology and Turbidity, *Food Hydrocolloids*

Nguyen, B. T., Nicolai, T., Chassenieux, C. & Benyahia, L. (2014), The effect of protein aggregate morphology on phase separation in mixtures with polysaccharides, *Journal of Physics: Condensed Matter*, **26**, 464102.

Nicolai, T. (2019), Gelation of food protein-protein mixtures, *Advances in Colloid and Interface Science*,**270**, 147-164

Soumpasis, D. M. (1983), Theoretical analysis of fluorescence photobleaching recovery experiments, *Biophysical journal*, **41**, 95-97.

Supplementary Information

Effect of Kappa Carrageenan on Acid-induced Gelation of Whey Protein Aggregates. Part II: Microstructure ,

Dasong Liu, Peng Zhou, Taco Nicolai

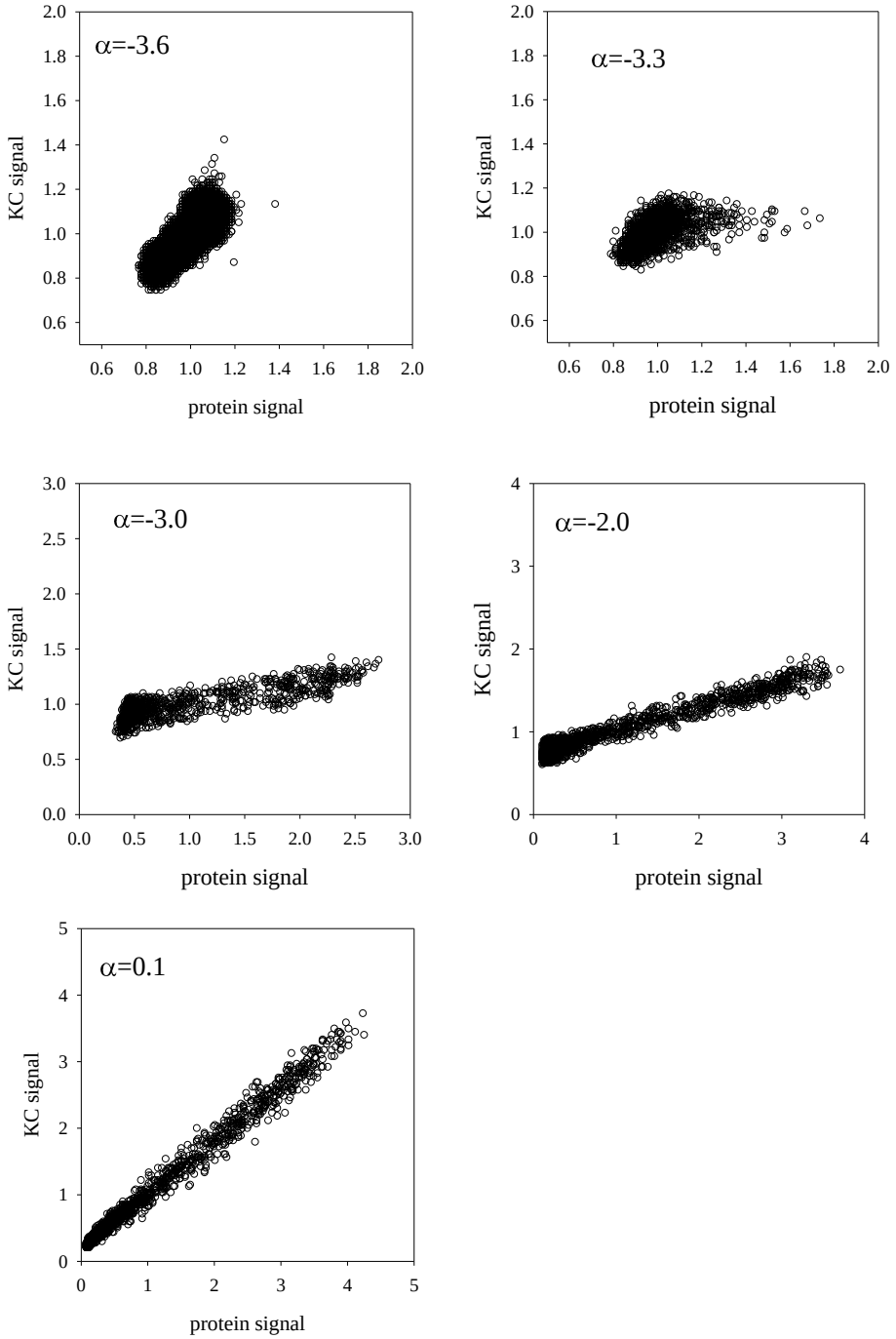

Fig. S1. Co-localization plots of the KC signal vs the protein signal normalized by the average intensity for mixtures of 20 g/L WPA and 2 g/L KC at different α. Notice the change in scale.

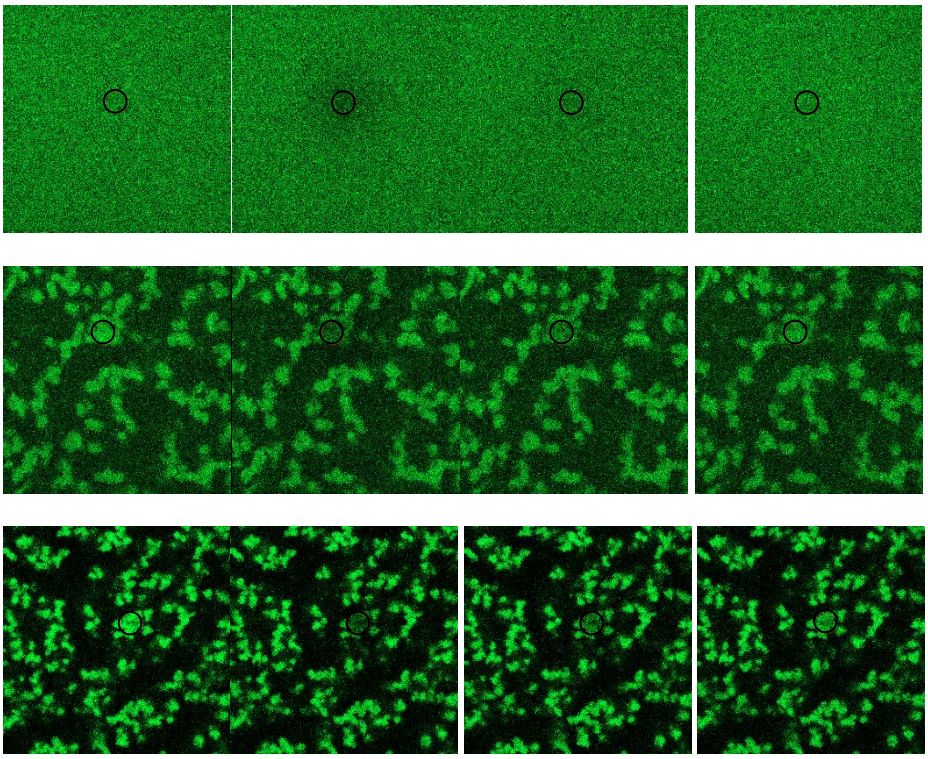

Fig. S2. CLSM images taken during FRAP measurements for mixtures of 20 g/L WPA and 2 g/L KC at different values of α indicated in the figure. The bleached area with diameter 10 µm is indicated by a black circle. The images from left to right were taken before bleaching, and 0.3 s, 33 s and 90 min after bleaching